PROCEEDINGS OF SCIENCE

PoS(ICHEP2016)679

LHCb results on Z forward-backward asymmetry and top cross section

---

X. Cid Vidal[*][†]
Universidade de Santiago de Compostela
E-mail: xabier.cid.vidal@cern.ch

By using proton-proton collision data of the LHC Run 1, LHCb measured the forward-backward charge asymmetry for the process $\bar{q}q \to Z/\gamma^* \to \mu^+\mu^-$. We will present these results, which provide the most precise measurement of the effective electroweak mixing angle at the Large Hadron Collider. The measurement of the inclusive top, $W+b\bar{b}$, $W+c\bar{c}$ and $t\bar{t}$ production cross sections, also performed with LHCb Run 1 data, will be presented too.

38th International Conference on High Energy Physics
3-10 August 2016
Chicago, USA

---

[*] Speaker.

[†] on behalf of the LHCb collaboration.

1. Introduction

LHCb is one of the four primary detectors of the Large Hadron Collider (LHC) project at CERN (Geneva, Switzerland). LHCb is a single-arm forward spectrometer with a unique coverage in terms of pseudo-rapidity, η, with a fully instrumented detector: $2 < \eta < 5$. While originally designed to study the production and decay of b and c hadrons, LHCb has extended its physics programme to also include other areas such as EW and top physics. Notable features of LHCb include precise integrated luminosity determination and an excellent secondary vertex reconstruction, lifetime and momentum resolution [1].

During Run 1 of LHC, LHCb recorded proton-proton collision data at centre of mass energies of $\sqrt{s} = 7$ TeV (2010 and 2011) and 8 TeV (2012). To optimise the performances for $b-$physics, LHCb runs with lower instantaneous luminosity than ATLAS and CMS, with the advantage of having stable conditions during a fill (thanks to the luminosity levelling) and low pile-up. LHCb recorded 1 fb^{-1} in 2011 and 2 fb^{-1} in 2012.

2. Forward-backward asymmetry in Z$\rightarrow\mu^+\mu^-$

The electroweak mixing angle θ_W is a fundamental parameter of the Standard Model (SM) electroweak lagrangian, providing a relationship between the masses of the W and Z bosons. In the SM, the coupling of the Z boson to fermions depends only on this angle. LHCb has determined the closely related effective angle [2], $\theta_\mathrm{W}^\mathrm{eff}$, by measuring the forward-backward asymmetry (A$_\mathrm{FB}$) in the decay $Z/\gamma^* \rightarrow \mu^+\mu^-$. This asymmetry is measured in the Collins-Soper frame [3] and an unfolding bayesian technique is applied to remove detector effects [4]. This includes correcting mainly for the efficiency of trigger, track reconstruction and potential detector mis-alignments. The measured asymmetry, obtained in bins of dimuon invariant mass, can be found in Fig. 1 for the 7 TeV and 8 TeV data samples.

In order to measure $\theta_\mathrm{W}^\mathrm{eff}$, a χ^2 comparison is made between A$_\mathrm{FB}$ predictions as a function of the di-muon mass for different values of $\sin^2(\theta_\mathrm{W}^\mathrm{eff})$. The χ^2 minimum sets the favoured value of

$$\sin^2(\theta_\mathrm{W}^\mathrm{eff}) = 0.23142 \pm 0.00073\ (\mathrm{stat.}) \pm 0.00052\ (\mathrm{syst.}) \pm 0.00056\ (\mathrm{th.})$$

where the experimental uncertainty is dominated by momentum biases originating from residual detector misalignment and the theoretical error is dominated by the parton distribution function (PDF) uncertainties. Fig. 2 shows the χ^2 obtained for different $\sin^2(\theta_\mathrm{W}^\mathrm{eff})$ hypotheses and compares the LHCb measurement to those from other experiments. The LHCb result is the most precise determination of $\sin^2(\theta_\mathrm{W}^\mathrm{eff})$ at the LHC. The reason for this is the fact that the forward-backward asymmetry is enhanced in the forward region due to a better knowledge of the direction of the colliding quark and anti-quark, consequently giving LHCb greater sensitivity to $\sin^2(\theta_\mathrm{W}^\mathrm{eff})$ than ATLAS and CMS.

3. Inclusive top production cross section

The measurement of the top production cross section in the forward direction can be used to constrain the gluon PDF at large momentum fraction [5]. The first top measurement at LHCb [6]

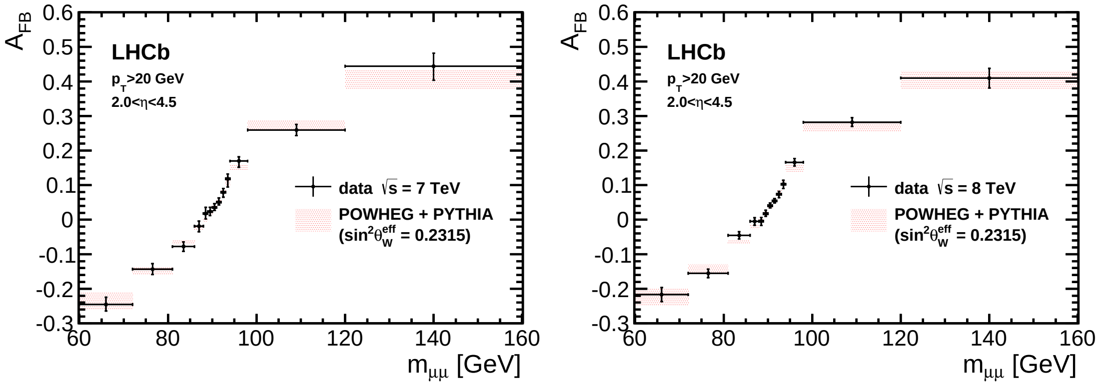

Figure 1: A$_{\rm FB}$ as a function of the di-muon mass, as measured by LHCb [2]. The left plot shows the measurement using the LHCb data taken at $\sqrt{s} = 7$ TeV, while the right one uses data taken at $\sqrt{s} = 8$ TeV. The SM prediction is also shown.

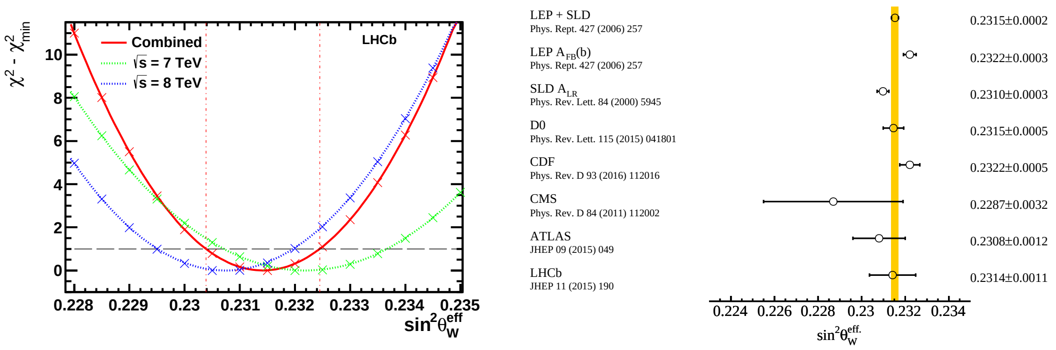

Figure 2: $\sin^2(\theta_{\rm W}^{\rm eff})$ measurements. Left, χ^2 showing the compatibility of LHCb data and different $\sin^2(\theta_{\rm W}^{\rm eff})$ hypotheses [2]. Right, comparison of $\sin^2(\theta_{\rm W}^{\rm eff})$ as measured by different experiments. The LHCb result is the most precise at the LHC.

has been performed in the $W+b$ final state, selecting events containing a high $p_{\rm T}$ isolated muon and a b jet. Jets are reconstructed using a particle flow algorithm [7] and clustered using the anti-$k_{\rm T}$ algorithm [8] with $\Delta R = 0.5$, with the b tagging of the jets achieved using the method described in [9].

The transverse component of the sum of the reconstructed b and muon momenta, $p_{\rm T}(\mu+b)$ can be used to discriminate between top and direct $W+b$ production, which is the main background for this search. Additional discrimination can be achieved using the charge asymmetry of the muons. Fig. 3 shows the number of candidates measured as a function of $p_{\rm T}(\mu+b)$ and the expected SM contribution from $W+b$ and top production. Top production is observed with a statistical significance of 5.4σ and the measured cross sections at $\sqrt{s} = 7$ TeV and 8 TeV

$$\sigma(\text{top})[7\text{ TeV}] = 239 \pm 53\text{ (stat.)} \pm 33\text{ (syst.)} \pm 24\text{ (th.) fb}$$
$$\sigma(\text{top})[8\text{ TeV}] = 289 \pm 43\text{ (stat.)} \pm 40\text{ (syst.)} \pm 29\text{ (th.) fb}$$

are compatible with the theoretical predictions within the experimental uncertainties. It should be mentioned that the $W+b$ and $W+c$ production cross sections were also measured by LHCb using the same dataset [10].

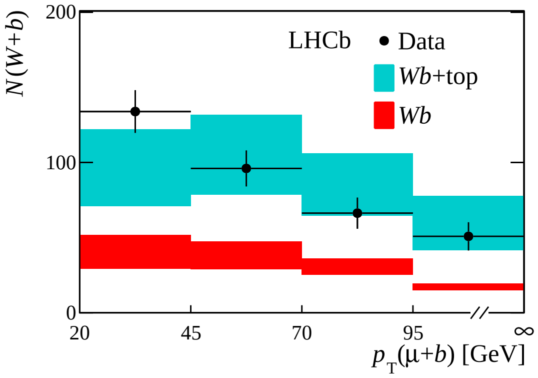

Figure 3: Number of candidates measured in LHCb $\sqrt{s} = 8$ TeV data as a function of $p_{\mathrm{T}}(\mu+b)$ in [6]. The expected SM contribution from $W+b$ and top production is also shown. Top production is observed with a statistical significance of 5.4σ.

4. $W+b\bar{b}$, $W+c\bar{c}$ and $t\bar{t}$ production cross sections

LHCb has measured the $W^{+}+b\bar{b}$, $W^{+}+c\bar{c}$, $W^{-}+b\bar{b}$, $W^{-}+c\bar{c}$ and $t\bar{t}$ production cross sections using a sample of pp collisions taken at $\sqrt{s} = 8$ TeV including a high-p_{T} lepton (electron or muon) and two heavy flavour (b or c) tagged jets [11]. The study of $W+c\bar{c}$ is the first of its kind.

In this analysis, jets are reconstructed as described in Sect. 3 and those coming from heavy quarks tagged using the method from [9]. The main backgrounds in this search are $Z+b\bar{b}$ and $Z+c\bar{c}$, single top and multi-jet QCD production. In order to extract the different signal components, a simultaneous 4-D fit is performed to the μ^{+}, μ^{-}, e^{+} and e^{-} samples. The four variables used in the fit are the dijet mass, a MVA-response to discriminate $t\bar{t}$ from $W+b\bar{b}$ and $W+c\bar{c}$ events (referred to as UGB, trained to be as uncorrelated as possible to the di-jet mass with the method described in [12]) and BDT$(b|c)$, a variable that separates b and c jets, also described in [9], used for both jets. Furthemore, in the fit only the signal components are floating, while the background is fixed to the SM theory expectations, with the exception of the QCD multi-jet background, which is extrapolated from a control sample in data. As an example, Fig. 4 shows the projections of this fit in the μ^{+} sample.

This analysis allows to observe the production of $W^{+}+b\bar{b}$, $W^{+}+c\bar{c}$, $W^{-}+b\bar{b}$, $W^{-}+c\bar{c}$ and $t\bar{t}$ with statistical significances of 7.1σ, 4.7σ, 5.6σ, 2.5σ and 4.9σ respectively. The cross sections measured in the LHCb fiducial region and the Next-to-Leading-Order (NLO) theory predictions can be found in Fig. 5.

This same dataset allows to perform the search for the SM Higgs boson decaying to a pair of $b\bar{b}$ or $c\bar{c}$ quarks and produced in association with a W or Z boson in LHCb. Details can be found in [13].

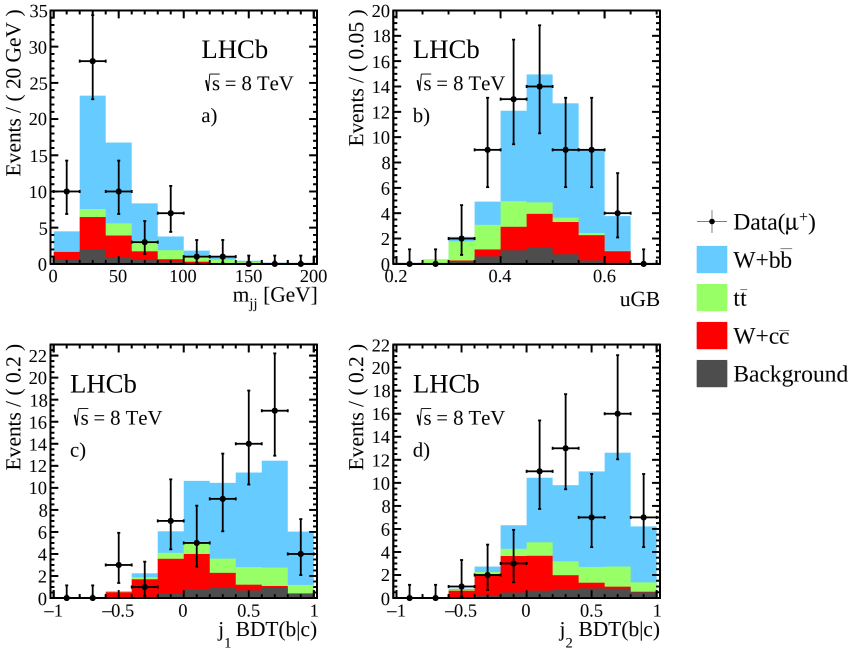

Figure 4: Example of the fit used to extract the production cross sections in [11]. Projections of the simultaneous 4D-fit results are shown for the μ^+ sample corresponding to: a) the dijet mass; b) the uGB response; the BDT$(b|c)$ of the c) leading and d) sub-leading jets.

5. Conclusions

Even though initially designed to measure flavour physics, LHCb now acts as a general purpose detector in the forward direction. Examples of this have been shown in terms of results in topics such as the measurement of $\sin^2(\theta_{\mathrm{W}}^{\mathrm{eff}})$, $W+b\bar{b}$, $W+c\bar{c}$ and different top production cross sections. The Run 2 of the LHC will extend the possibilities of LHCb beyond flavour physics. As a significant example of this, a factor of 20 increase in the top yield at the end of Run 2 is expected.

References

[1] LHCb, R. Aaij *et al.*, *LHCb Detector Performance*, Int. J. Mod. Phys. **A30** (2015), no.~07 1530022, `arXiv:1412.6352`.

[2] LHCb collaboration, R. Aaij *et al.*, *Measurement of the forward-backward asymmetry in $Z/\gamma^* \to \mu^+\mu^-$ decays and determination of the effective weak mixing angle*, JHEP **11** (2015) 190, `arXiv:1509.07645`.

[3] J. C. Collins and D. E. Soper, *Angular distribution of dileptons in high-energy hadron collisions*, Phys. Rev. D **16** (1977) 2219.

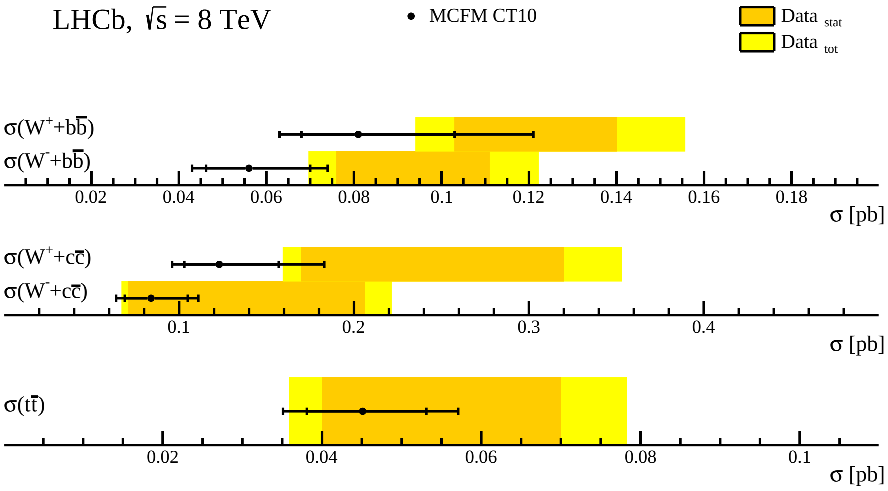

Figure 5: Graphical display of the measured $W\!+\!b\bar{b}$, $W\!+\!c\bar{c}$ and $t\bar{t}$ production cross sections and the corresponding NLO theoretical SM predictions [11]. The outer bars (light yellow) correspond to the total uncertainties of the measured cross-sections and the inner bars (dark yellow) correspond to the statistical uncertainties. Theoretical prediction is represented by the black markers and error bars, where inner and outer uncertainties represent the scale and the total errors respectively.

[4] G. D'Agostini, *A Multidimensional unfolding method based on Bayes' theorem*, Nucl. Instrum. Meth. **A362** (1995) 487.

[5] R. Gauld, *Feasibility of top quark measurements at LHCb and constraints on the large-x gluon PDF*, JHEP **02** (2014) 126, `arXiv:1311.1810`.

[6] LHCb collaboration, R. Aaij *et al.*, *First observation of top quark production in the forward region*, Phys. Rev. Lett. **115** (2015) 112001, `arXiv:1506.00903`.

[7] LHCb collaboration, R. Aaij *et al.*, *Study of forward Z+jet production in pp collisions at* $\sqrt{s} = 7$ *TeV*, JHEP **01** (2014) 033, `arXiv:1310.8197`.

[8] M. Cacciari, G. P. Salam, and G. Soyez, *The Anti-k(t) jet clustering algorithm*, JHEP **04** (2008) 063, `arXiv:0802.1189`.

[9] LHCb collaboration, R. Aaij *et al.*, *Identification of beauty and charm quark jets at LHCb*, JINST **10** (2015) P06013, `arXiv:1504.07670`.

[10] LHCb collaboration, R. Aaij *et al.*, *Study of W boson production in association with beauty and charm*, Phys. Rev. **D92** (2015) 052012, `arXiv:1505.04051`.

[11] LHCb, R. Aaij *et al.*, *Measurement of forward* $t\bar{t}$*,* $W+b\bar{b}$ *and* $W+c\bar{c}$ *production in pp collisions at* $\sqrt{s} = 8$ *TeV*, `arXiv:1610.08142`, Submitted to Phys. Lett. B.

[12] A. Rogozhnikov *et al.*, *New approaches for boosting to uniformity*, JINST **10** (2015) T03002, `arXiv:1410.4140`.

[13] LHCb Collaboration, *Search for* $H^0 \to b\bar{b}$ *or* $c\bar{c}$ *in association with a W or Z boson in the forward region of pp collisions*, Tech. Rep. LHCb-CONF-2016-006. CERN-LHCb-CONF-2016-006, CERN, Geneva, Sep, 2016.